TISSUE ENGINEERING: Part A
Volume 00, Number 00, 2019

DOI: 10.1089/ten.tea.2018.0277

termis
Tissue Engineering
& Regenerative Medicine
International Society

Tissue-Engineered Esophagus via Bioreactor Cultivation for Circumferential Esophageal Reconstruction

In Gul Kim, PhD,[1,*] Yanru Wu, MS,[2,*] Su A. Park, PhD,[3] Hana Cho, MS,[1] Jun Jae Choi, BS,[1] Seong Keun Kwon, MD, PhD,[1] Jung-Woog Shin, PhD,[2,*] and Eun-Jae Chung, MD, PhD[1,*]

The use of biomaterials for circumferential esophageal repair is technically challenging in a rat model, and an optimal scaffold implantation technique with nutritional support is essential. The purpose of this study was to investigate the effects of three-dimensional printed esophageal grafts and bioreactor cultivation on muscle regeneration and reepithelialization from circumferential esophageal defects in a rat model. Here, we designed an artificial esophagus that can enhance the regeneration of esophageal mucosa and muscle through the optimal combination of a two-layered tubular scaffold and mesenchymal stem cell-based bioreactor system. The graft was verified by the performance comparison with an omentum-cultured esophageal scaffold. We also applied a new surgical anastomosis technique and a thyroid gland flap over the implanted scaffold to improve graft survival. Although no regenerated mucosal layer was observed around the implants of the control group, histological examination of the regenerative esophagi along the scaffold revealed that the bioreactor system and omentum-cultured groups showed more than 80% of the mucosal regeneration without a fistula. The regenerated tissues showed that the integration of the esophageal scaffold and its native esophageal tissue was intact and were covered with layers of stratified squamous epithelium with several newly developed blood vessels. Therefore, this study describes a novel approach for circumferential esophageal reconstruction.

Keywords: esophageal reconstruction, 3D printing, scaffold, bioreactor

Impact Statement

In vivo functional esophageal reconstruction remains challenging due to anastomosis site leakage and necrosis of the implanted scaffold in a circumferential esophageal defect. Therefore, it is necessary to develop a tissue-engineered esophagus that enables regeneration of esophageal mucosa and muscle without leakage of the esophageal anastomosis. In this study, we proposed an intriguing strategy that combines a mesenchymal stem cell-seeded tubular scaffold with a bioreactor system for esophageal reconstruction and introduced a new surgical anastomosis technique with the thyroid gland flap over the implanted scaffold to improve graft survival. We believe that this system should be a powerful platform for circumferential replacement of the esophagus in a rat model.

Introduction

The treatment of esophageal disorders, such as congenital anomalies and esophageal cancer, results in circumferential, full-thickness, extended segment loss of the esophagus. Gastric pull-up conduits or colon interpositions are used to reestablish the luminal continuity. However, the use of these esophageal substitutes can cause various surgical morbidities and mortality.[1,2] Hence, esophageal tissue engineering could be emerging as promising alternative strategies to develop a mimic of each patient's native esophagus.[3,4] Although tissue engineering promises to be an effective regenerative strategy, there is a lack of positive evidence to replace a circumferential esophageal defect. The use of biomaterials for circumferential esophageal repair is technically challenging, and significant expertise is required to perform surgical procedures and postoperative nutritional care, particularly in the murine esophagus.[5]

[1]Department of Otorhinolaryngology-Head and Neck Surgery, Seoul National University, College of Medicine, Seoul, Republic of Korea.
[2]Department of Biomedical Engineering, Inje University, Gimhae, Republic of Korea.
[3]Department of Nature-Inspired Nanoconvergence Systems, Korea Institute of Machinery and Materials, Daejeon, Republic of Korea.
*These authors contributed equally to this work as first and corresponding authors.

The small size of the rat esophagus and lack of peristaltic activity after nondynamic scaffold implant likely prevent normal esophageal swallowing. Although the scaffold exhibits complete healing of the circumferential defects in the rat model, most animals die before the second postoperative week.[5,6] The deaths occurred due to stenosis, graft obstruction by foreign material (hair by grooming), and malnutrition. Moreover, anastomosis site leakage inevitably causes extremely high mortality because of neck and mediastinal contamination, which results in sepsis or adjacent airway edema and obstruction.

Therefore, the engineered scaffold should have characteristics similar to the native organ, and an optimal scaffold implantation technique with nutritional support is necessary in the rat model. The viscoelasticity of the implanted esophagus should be adequate for the repetitive ramp-relaxation of the peristaltic movement through the esophagus. The dilatation and burst strength of the scaffold should match the native esophagus because it should not leak or shrink.[7,8] From the technical perspective of surgery and postoperative care, watertight anastomosis is essential to prevent leakage, and a postoperative alternative feeding route such as a nasogastric tube should be considered to prevent food or saliva contamination at the anastomosis site with optimal nutrition. Once the artificial tissue structure is transplanted *in vivo*, a reliable vascular vehicle is required during this initial stage.[9]

To overcome these problems, we fabricated a novel two-layered tubular scaffold as an artificial esophagus consisting of electrospun nanofibers (inner layer) and three-dimensional (3D) printed strands (outer layer) (Fig. 1A). Human adipose-derived mesenchymal stem cells (hMSCs) were seeded onto the inner layer of the scaffold to promote reepithelialization (Fig. 1B). We hypothesized that the inner nanofiber structure can act as a template for the mucosal layer by providing topographical cues for cell migration and that the 3D printed strand (outer) can provide mechanical strength and flexibility as the framework of the esophagus. To achieve full regeneration of the esophageal mucosa and muscle layer, further bioactivity for esophageal reconstruction was conferred to this scaffold through bioreactor cultivation as well as coverage of the thyroid gland flap on the implanted scaffold (Fig. 1C). We also compared the efficacy of bioreactor systems with the performance of existing omentum-cultured scaffolding technology (Fig. 1D).[10]

Therefore, the purpose of this study was to evaluate the potential of a bioreactor system and a surgical technique,

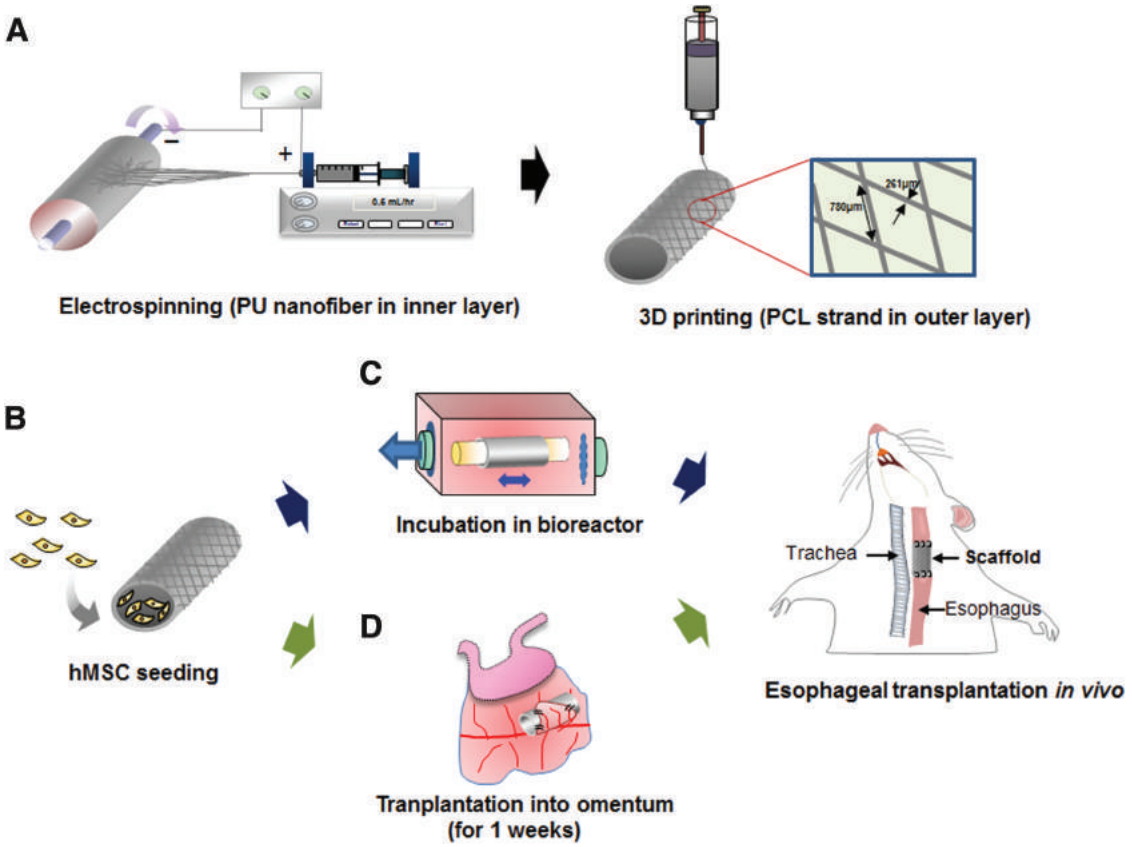

FIG. 1. Schematic illustration of the process used to fabricate two-layered tubular scaffolds and esophageal transplantation including tissue-engineered technique thereon. **(A)** The first step involved the fabrication of the inner membrane of the scaffold by electrospinning using PU. After fabricating the inner membrane by electrospinning, the structural strength of the tubular scaffold was reinforced by adding strands to the outer surface of the membrane using a 3D printing system without solvent. **(B)** hMSCs (encapsulated in Matrigel®) were seeded onto the inner layers of the two-layered tubular scaffold. These scaffolds were incubated into bioreactor system **(C)** and omentum tissue **(D)**, respectively, and then, the tissue-engineered esophaguses were implanted into the cervical esophagus. hMSCs, human adipose-derived mesenchymal stem cells; PU, polyurethane. Color images are available online.

including thyroid gland flap and esophageal anastomosis, using a tissue-engineered scaffold that was developed by combining a 3D printed reinforcement framework in a rat model for circumferential esophageal reconstruction.

Materials and Methods

Preparation of the hybrid esophageal tube

Biotubular esophageal scaffolds were fabricated by combining electrospinning and 3D printing. First, the inner membrane of the tubular scaffold was fabricated by electrospun polyurethane (PU; Pellethane, Lubrizol) with rotating stainless steel mandrels (diameter = 2 mm) as the collector that had been described previously.[11] Briefly, the PU polymer was dissolved in N,N-dimethylformamide (DMF; Junsei Chemical Co., Japan) by stirring at room temperature for 8 h, resulting in a 20% (w/v) solution. The working distance between the needle tip and rotating collector was set to be 30 cm, where 15 kV was engaged by a power supply (SHV200 RD-40k; Convertech, Korea). The feeding rate was set to 0.5 mL/h. The linear speed of the outer surface of the rotating collector was 3.14 m/s. The nanofibers were collected on the surface of the rotating mandrels. After fabricating the inner membrane by electrospinning, the structural strength of the tubular scaffold was reinforced by adding strands to the outer surface of the membrane using a 3D printing system, without a solvent, as described previously.[12] Briefly, PCL (polycaprolactone; Sigma) polymer was melted in a heating cylinder, and then, strands were squeezed out by high pressure ($\sim$7 bar) under the control of a bioplotting system (EnvisionTEC, Germany). Finally, this two-layered scaffold was removed from the mandrel, and a hollow tubular structure was acquired. They were also sterilized by soaking in 70% ethanol under ultraviolet light.

Characterization

The tubular scaffolds were visualized using a scanning electron microscopy (SEM; Model S-3000N; Hitachi, Japan). Before scanning, all the scaffolds were sputter-coated with gold, and the accelerating voltage was set at 5 kV to view the surface morphologies. The average fiber and pore size of the scaffolds were estimated from the SEM digital images obtained by ImageJ software (NIH) according to the scale bar in the image and the proportion between the fiber/pore size and scale bar. Thirty measurements were examined over five tubular scaffolds, and the results are expressed as the means ± standard deviation.

Mechanical test

A compliance test was carried out to evaluate the mechanical properties of the fabricated tubular scaffolds. While the intraluminal pressure was increased, the changes in the external diameter of the tubular scaffold were measured by digital image processing. Briefly, the pressure was applied using a 50-mL syringe pump and monitored with a digital pressure gauge (ZSE50F; SMC Korea). Before performing the compliance test, the scaffolds were preconditioned with 100 mmHg intraluminal pressure by injecting phosphate-buffered saline (PBS; Sigma–Aldrich) into the tubular scaffolds three times. Next, PBS was slowly ($\sim$10 mmHg/min) injected into the scaffolds to produce a pressure up to 100 mmHg. The recorded images were analyzed by the ImageJ (NIH) to calculate the changes in their diameter. Finally, the compliance (C) of the scaffold was evaluated based on the equation of $C = (\Delta D/D_o)/P$, where D_o is the original external diameter of the tube, ΔD is the change in the external diameter, and P is the pressure. Note that the increment of pressure was based on $P = 0$ mmHg. The tensile stress of 3D printed/nanofiber scaffolds was measured using an ultimate tensile test machine (AG-5000G; Shimadzu, Japan) equipped with a 10-kgf load cell at a crosshead displacement speed of 20 mm/min. The esophagus of a normal rat was used as a control group. Specimens were prepared in 2 cm lengths and fixed to the grips at 5 mm on both ends of the sample ($n = 4$).

Dynamic cultivation of the hMSC-seeded tubular scaffold

Once the 3D printed esophageal scaffolds were prepared, they were sterilized under ultraviolet light for 1 h, prewet with ethanol for 10 min, and washed three times in PBS. Human adipose-derived mesenchymal stem cells (hMSCs, R7788-110; STEMPRO®), purchased from Gibco™, were used without modification (Passage No. 3). To achieve efficient attachment on the inner surface of the scaffold, dissociated hMSCs were suspended at a density of 1×10^6 cells/mL in Matrigel (354234; Corning) containing growth medium (MesenPRO RS™, Basal Medium/Growth supplement), and the suspension was then applied in an even coating on the inner surfaces of the scaffolds. Cell-seeded scaffolds were tightly fitted into acrylic holders in the culture chambers of a custom-made bioreactor. The culture chamber was then filled with growth medium, and 0.1 dyne/cm^2 flow-induced shear stress with a pattern of 1 min/2 min for engagement/resting was applied at 37°C under a humidified atmosphere with 5% CO_2 (Supplementary Table S1). Cell viability on the two-layered tubular scaffold (inner surface) without dynamic culture was determined after 5 days using a LIVE/DEAD® Viability Assay Kit (Molecular Probes) according to the manufacturer's instructions. Images were obtained via confocal microscopy (LSM510 META; Carl Zeiss) using the z-stack tool. Cell proliferation was analyzed on days 1, 3, and 7 using a CCK-8 assay (Dojindo, Japan) without a bioreactor system. A 10% CCK-8 solution was added to the prepared sample and incubated at 37°C for 2 h. Aliquots from each sample (100 mL) were transferred into a 96-well plate, and their absorbance was measured at a wavelength of 450 nm using a Multiscan microplate reader (Thermo Scientific). The surface morphology of the hMSC-seeded scaffolds on day 3 was observed by SEM operated at an accelerating voltage of 25 kV. Before the evaluation of the morphology, the hMSCs on the cross-sectioned tubular scaffold were fixed with 2.5% glutaraldehyde (Sigma) and OsO_4 (Sigma) for 24 h, followed by ethanol dehydration. The fixed hMSCs in scaffold specimens was coated with platinum using a sputter coater (SC 7680; Quorum Technologies, United Kingdom) under argon atmosphere conditions.

Animal Study

Orthotopic esophageal scaffold implantation into the cervical esophagus

After 1 week of gastrostomy, the hybrid esophageal scaffold implantation was performed. Detailed surgical procedures for

T-tube insertion-gastrostomy are described in Supplementary Materials and Methods. To facilitate the penetration of blood vessels and tissues, they were transplanted into the omentum of a rat model for 1 week. Before transplantation, the hMSCs (cell density: 1×10^6 cells/mL in Matrigel) were inoculated into the inner wall of each scaffold and were incubated in the bioreactor system for 3 days. Adult Sprague-Dawley rats (Orient Bio, Seoul, Korea) that weighed 398 to 420 g for esophageal transplantation were used in the study. The animals were divided into five groups ($n = 7$ per group) as follows: (1) implantation of the naked scaffold (control), (2) coverage of the thyroid gland flaps after scaffold implantation (flap), (3) coverage of the thyroid gland flaps after the implantation of hMSC-seeded scaffolds (mesenchymal stem cell [MSC]), (4) implantation with thyroid gland flap after omentum culture of hMSC-seeded scaffolds (omentum), and (5) implantation with thyroid gland flap after bioreactor culture of hMSC-seeded scaffolds (bioreactor). The surgical procedure was as follows. The neck was shaved, and standard draping of surgical site was performed for aseptic surgery. A ventral midline incision was made, and the strap muscle was divided to isolate the tracheoesophageal structure. Left-side esophagus isolation was performed under a magnified view, and the upper part was dissected from the thyroid gland carefully. A 5-mm-long full circumferential defect including all layers of the esophagus was created. The circumferential esophageal defects were orthotopically reconstructed by a scaffold with a 9-0 nylon suture (Johnson & Johnson Co., Norderstedt, Germany) for the proximal and distal anastomoses under a microscope. The first suture was placed between the right inferoposterior margin of the remnant upper esophagus and scaffold. Consecutive serial sutures were placed from the right to left side between the remnant upper esophagus and scaffold. The upper margin of the remnant lower esophagus was anastomosed with the scaffold in the same manner (Supplementary Movie S1). The implanted scaffold was covered on one side with the thyroid gland. The muscle and skin tissues were closed with a 4-0 Vicryl suture. All animals were housed in individual metabolic cages obtained from our animal facility. This study was carried out in strict accordance with the guidelines of the Animal Research Committee, Seoul National University Hospital. All protocols and experimental design parameters were reviewed and approved by the Institutional Animal Care and Use Committee of the Seoul National University Hospital (approval number: 17-0164-S1A0).

Evaluation of the postoperative clinical course

The rats were injected with the daily antibiotic gentamicin (20 mg/kg) (Septopal®). Oral liquid feeding was started on the third day after the surgery until the end point of the study, and the entire nutrition formula (20.6 g/100 mL [g%] carbohydrate, 3.8 g% protein, and 0.2 g% fat) was supplied through the gastrostomy site three times per day beginning the day after the surgery.[13]

Postoperative monitoring was performed daily of the animal's survival and weight, assessing respiratory and dietary conditions, behavior, such as self-harming incision site or resistance to tube intake, as well as the occurrence of surgical complications. Moreover, the rats were evaluated by one of the authors for appearance and attitude according to a 5-point scale (Supplementary Table S2).[14] Particularly, when the body weight of the rat models decreased rapidly by 20% or more, we consulted with the veterinarian to determine euthanasia.

Blood parameters

We collected blood samples in ethylenediaminetetraacetic acid (EDTA) anticoagulant bottles on the postoperative 7th and 14th days. Various blood parameters (blood urea nitrogen [BUN], white blood cells [WBCs], hemoglobin [Hgb], albumin [Alb]) were analyzed in the experimental and normal control groups ($n = 3$). Biochemical tests (BUN and Alb) were performed using a Hitachi 7180i Autoanalyzer (Hitachi High-Technologies Corporation, Japan). The complete blood count (WBC and Hgb) was determined using a hematology autoanalyzer-ADVIA2120i (Siemens Healthcare Diagnostics, Inc.). All samples were analyzed within 30 min of collection. Each analysis was performed following the manufacturer's operational guidelines.

Histological examination

The autopsy was performed under the microscopic view after the natural death of the rat. The inside and outside of the grafts were evaluated, and the grafts with the sections of adjacent esophageal tissue were fixed in 4% paraformaldehyde, embedded in paraffin, and sectioned serially into 4-μm-thick sections in the sagittal plane from the base of the tongue to the end of the cervical esophagus. The sections were deparaffinized and dehydrated in a graded series of ethanol. The histological sections were stained with hematoxylin and eosin (H&E) and Masson's trichrome, following standard histological techniques to evaluate the regeneration process of the esophageal defect. Elastin was also stained using the Elastic (Modified Verhoff's) stain kit (ES4807) according to the manufacturer's instructions. Histological images were obtained in triplicate for each group using a light microscope (Olympus, Japan).

Immunohistological analysis

For immunohistochemistry, endogenous peroxidase was inactivated using 3% hydrogen peroxide in methanol for 30 min. The tissue sections were washed with PBS and then were exposed to 3% bovine serum albumin to block nonspecific reactions. The sections were subsequently incubated with anti-keratin 13 (1:50 dilution; mouse monoclonal antibody; ABIN126702) and anti-desmin (1:200 dilution; rabbit polyclonal antibody; Abcam, United Kingdom) along with the secondary antibodies Alexa Fluor 594 goat anti-mouse (ab150116; Abcam) and Alexa Fluor 488 goat anti-rabbit (ab150077; Abcam), respectively. Reepithelialization was calculated as a percentage of the specific expressed length versus the transplanted length ($n = 6$). Muscle regeneration was also calculated from the fluorescence distribution of the desmin-positive area at the transplanted site using the ImageJ software ($n = 6$). Tissue sections for F4/80 (1:200 dilution; mouse monoclonal antibody; Abcam) and von Willebrand factor (vWF) (1:200 dilution; rabbit monoclonal antibody; Abcam) were then incubated using the horseradish peroxidase-conjugated kit (Vectastain®) and then were visualized using 3,3′-diaminobenzidine (DAB) (Vector, pk-7800). Cell nuclei were counterstained with hematoxylin. Primary antibody (mouse monoclonal anti-human nuclei PMAB1281;

EMD Millipore) and secondary antibody (Alexa Fluor 594 goat anti-mouse; ab150113) were also administered to track the presence of transplanted human cells. The number of vWF-positive blood vessels and F4/80-positive macrophages was quantified using the ImageJ. Five areas (200× magnification) were examined per slide ($n=6$ per group) by a blinded observer. Images were captured using a fluorescence microscope (BX43-32FA1-S09; Olympus Optical, Japan).

Statistical analysis

The data are expressed as the means ± standard deviation. Statistical significance was determined via one-way analysis of variance (ANOVA) with Tukey–Kramer's *post hoc* test (GraphPad Prism 5; GraphPad Software, La Jolla, CA). Statistical significance was marked as $*p<0.05$, $**p<0.01$, and $***p<0.001$.

Results

Characterization of artificial esophageal scaffolds

Tubular scaffolds were manufactured, and their surface morphologies were observed and analyzed by SEM. It was observed that the tube wall had an asymmetric column-shaped fiber structure (Fig. 2A). The inner surface of the tube had electrospun nanofibers, which can effectively induce the mucosal layer and improve cell migration, whereas

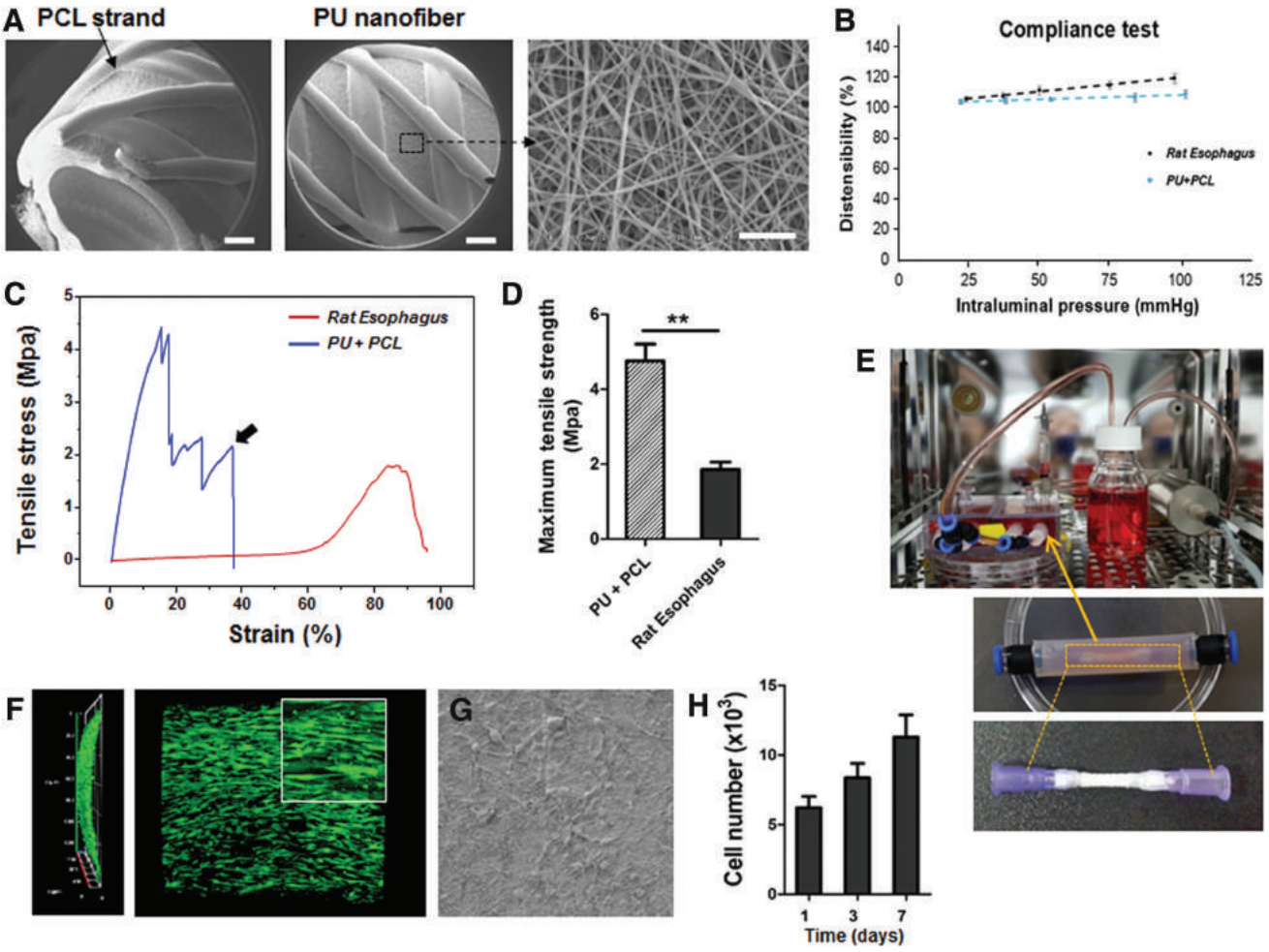

FIG. 2. Characterization and dynamic culture of two-layered tracheal scaffolds. **(A)** SEM images of the esophageal scaffold. Overview of the two-layered tubular structure of scaffold; (*left*) the end of PCL/PU tubular scaffold (scale = 500 μm), (*middle*) the outer surface of PCL strand (scale = 500 μm), and (*right*) nanofiber-based structure of the scaffold with highly porous structure (scale = 10 μm). **(B)** Compliance test of the esophageal scaffold. The changes of external diameter in native rat esophagus and tubular scaffold were measured following increased intraluminal pressure ($n=3$). **(C)** Maximum tensile strength of the two-layered esophageal scaffold before transplantation. The *arrow* indicates the breaking point of the inner PCL nanofibers. **(D)** PU+PCL tubular scaffold had significantly higher tensile strength than native esophagus ($**p<0.01$). **(E)** Dynamic culture of the two-layered tracheal scaffold using custom-made bioreactor device. Each scaffold immersed in medium is exposed to a fluid flow-induced shear stress. **(F)** Live/dead staining to analyze cell viability on the two-layered tubular scaffold (luminal surface) indicates that most cells are viable, and they spread quite well on nanofiber structure in 5 days (scale = 100 μm). **(G)** SEM images showed that the hMSCs were adhering and spreading on the surface of the PU/PCL nanofiber after 3 days of culture (scale = 100 μm). **(H)** hMSC proliferation is examined on inner layer of the scaffold groups on days 1, 3, and 7 via the CCK-8 metabolic assay ($n=5$). PCL, polycaprolactone; SEM, scanning electron microscopy. Color images are available online.

the outer surface had microsize fibers, which can provide mechanical strength and flexibility. The width of the 3D printed strands, which were directly attached to the inner membrane, averaged 540 μm. The thicknesses of the inner and outer layers in the scaffold were 192 ± 18 and 268 ± 31 μm, respectively. The diameters of the inner and outer layers in the scaffold were an average of 2.05 ± 0.25 and 2.38 ± 0.28 mm, respectively (Table 1). In particular, the diameter of the inner electrospun fibers averaged 517 ± 319 nm. Compliance tests were performed to evaluate the mechanical property of the suggested tubular scaffold and native rat esophagi. Figure 2B shows that the diameter expands linearly with the increasing intraluminal pressure in both cases. The compliance values of each case were $0.108 \pm 0.036\%$/mmHg ($n = 3$) and $0.207 \pm 0.016\%$/mmHg ($n = 3$) for the scaffold and native rat esophagus, respectively. To investigate the intrinsic mechanical properties of the two-layered tubular scaffold and native esophagus of rats, we conducted a direct tensile test on the whole scaffold (Fig. 2C). When pulling at 20 mm/min speed, 3D printed PCL strand constituting outer layer keeps up with maximum stress and fractured at the stress of 4.5 Mpa. After that, some remaining PCL strands are supported by the tensile stress and are then broken at 28% strain value. Finally, the PU nanofibers constituting the inner wall support tensile force but rupture at a strain value of 38% (indicated by arrows). The maximum tensile strength of the 3D printed strands supporting the outer wall was significantly different from that of the esophageal tissue (Fig. 2D). However, the tensile stress of the nanofiber layer on the inner wall was similar to that of the normal esophagus. Nevertheless, there was a marked difference in elongation between the two groups. These results suggest that the native esophagus is much more stretchable for peristalsis than the artificial scaffold.

Dynamic culture of hMSCs on two-layered artificial esophagi

We used a 3D dynamic culture system to enhance the epithelial differentiation of MSCs in the two-layered tubular scaffold before *in vivo* transplantation. A custom-made bioreactor was fabricated according to the dimensions appropriate for the cultivation of small sized-tubular scaffolds (Fig. 2E). We have already investigated proper shear stress for the engraftment of hMSCs on the inner part of this scaffold through previous studies and evaluated the differentiation potential into epithelial cells under various differentiation markers.[15] Therefore, this study focuses on whether hMSCs attach uniformly to the inner wall of the tubular scaffold. The cytotoxicity of the tubular scaffold itself was also evaluated by the CCK-8 assay without dynamic culture. After uniform cell attachment to the cylindrical scaffold, cells were monitored for 7 days. Live/dead staining was used to analyze cell viability on the two-layered tubular scaffold (luminal surface) at 5 days and showed that most cells were viable and spread well on the nanofiber structure, indicating a favorable environment provided by the topographical cues of the nanofibers (Fig. 2F). The images were processed with a confocal z-stack, and hMSCs were observed to be fully proliferated in a portion of the cylindrical scaffold. The morphology of the hMSCs grown with culture on the inner layer of the scaffold is shown in Figure 2G. These data showed that the hMSCs were well integrated with the nanofiber structure and showed high cell engraftment under growth medium. The CCK-8 assay confirmed that MSC proliferation increased over time on the nanofiber structure (Fig. 2H).

Esophageal transplantation and a postoperative clinical course

We performed tube-inserted gastrostomy on all animal models to allow survival without oral feeding before transplantation (Fig. 3A). The relevant data are shown in Supplementary Figure S1. All animals that underwent T-tube gastrostomy exhibited rapid weight loss within a week, but then, the weight remained constant (Supplementary Fig. S1A). After 4 weeks of the gastrostomy procedure, all rats were successfully intubated into the gastric wall (Supplementary Fig. S1B). Tube-inserted gastrostomy, which has been successfully tested until 4 weeks, has been commonly applied to all rats before esophageal transplantation. All esophageal transplantations were performed 1 week after gastrostomy. Each hMSC-seeded tubular scaffolds, including omental tissue culture and bioreactor cultivation, were transplanted at full circumferential esophageal defects via microsuture techniques (Supplementary Movie S1). Figure 3B indicates representative images of esophageal transplantation under the microscope. The graft was covered with a thyroid gland flap for stable fixation and vascular supply of the implanted site. Separately, hMSC-seeded tubular scaffolds were implanted into the omentum to embed blood vessels around the grafts (the omentum group; Fig. 3C). One week after implantation, omentum-transplanted specimens were thickly covered with tissue embedded with blood vessels.

The surgical procedure was successfully completed in seven rats per group, and there were three unexpected deaths (peritonitis after gastrostomy, $n = 1$; death during implantation of the control group, $n = 1$; unknown cause of death at 1 day after implantation of the MSC group). The control group was reduced up to 300 g of their weight at the end of the first week (Fig. 3D). Then, their weight decreased rapidly up to 240 g, and they did not survive beyond 9 days. However, survival was significantly higher in all the experimental groups covered with thyroid gland than in the control group (Fig. 3E). The weight of most of the flap group also did not decrease below 320 g at 7 days after the surgery. The bioreactor group and the omentum group were maintained at ~ 340 g until day 9. Thereafter,

Table 1. Characteristics of the Polyurethane/Polycaprolactone Scaffold Reinforced by a Three-Dimensional Printed Outer Ring

	Thickness of inner layer (μm)	*Thickness of outer layer (μm)*	*Inner diameter of scaffold (mm)*	*Outer diameter of scaffold (mm)*
Mean ± SD	192 ± 18	268 ± 31	2.05 ± 0.25	2.38 ± 0.28

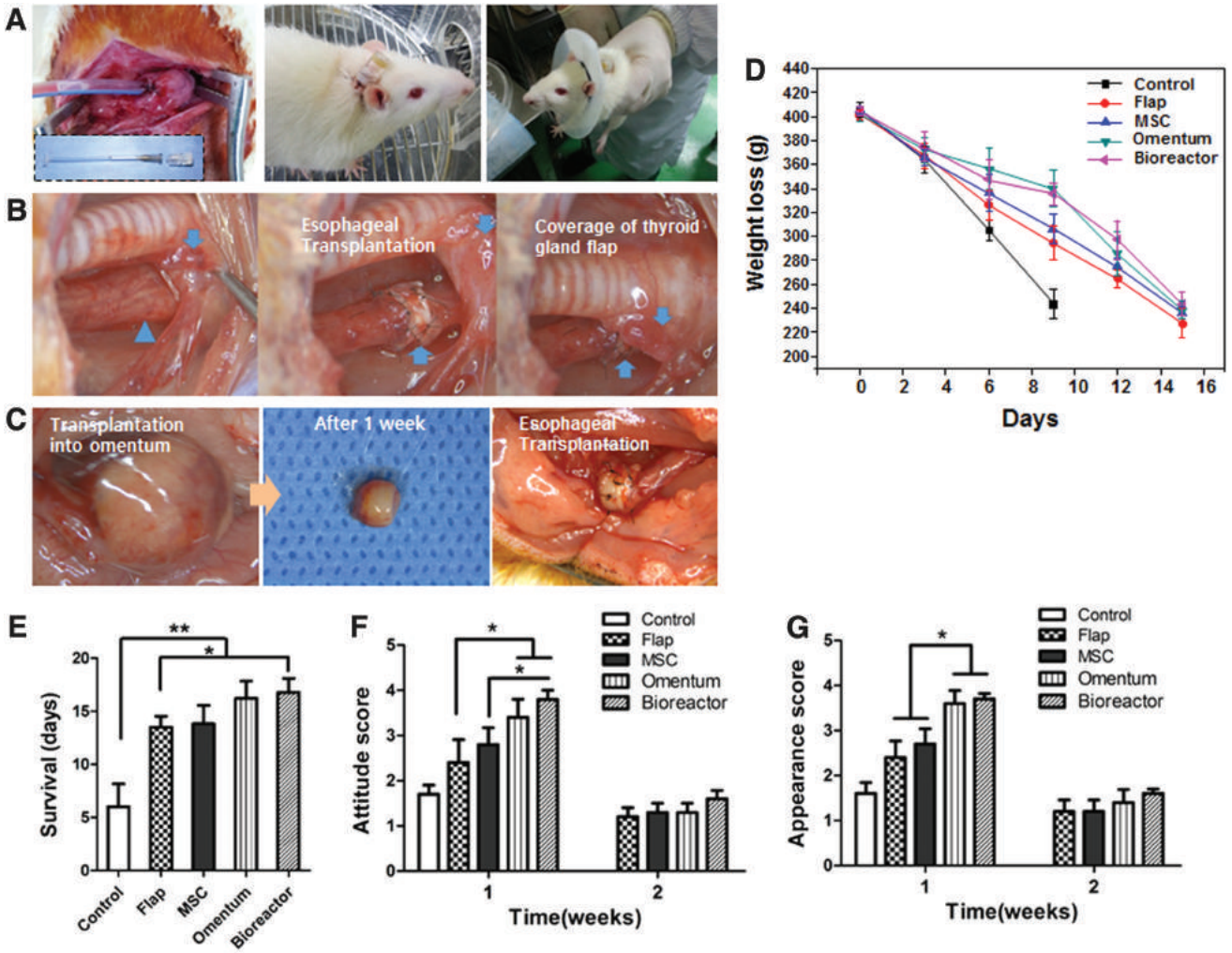

FIG. 3. Esophageal transplantation and postoperative nutritional grading. **(A)** T-tube insertion into a rat stomach for rat survival without oral feeding. The tube was pulled through from a tunnel under the skin and fixed to the dorsal skin. A heparin cap was used to prevent the gastric contents from flowing backward. Neck collar was then applied to prevent self-harming of the device. **(B)** Orthotopic esophageal scaffold implantation into the cervical esophagus. The upper esophagus was dissected from the thyroid gland (*blue arrow*) carefully. *Blue arrowhead* indicates sites of circumferential defect of normal esophagus. A 1 cm full circumferential defect including all layers of the esophagus was created and reconstructed by scaffold under a microscope. The implanted scaffold was covered on one side with the thyroid gland to improve blood supply. **(C)** The esophageal scaffold was embedded into the lower portion of the omentum and wrapped using 4-0 Vicryl sutures. After 1 week of implantation, the cultured scaffold was harvested and immediately transplanted into the cervical esophagus. **(D)** Weight loss studies after esophageal transplantation. Weight loss was determined as absolute change from initial weight of each group. **(E)** The survival rate of all the experimental groups covered with the thyroid gland flap was significantly higher than that of the control group. A physical condition evaluated by the **(F)** attitude and **(G)** appearance and grading scores. ($*p<0.05$ or $**p<0.01$). Color images are available online.

most of the rats died at ~15 days due to sudden weight loss that was associated with various causes. This tendency was indicated by the physical condition (appearance and attitude grade score). The score was blindly evaluated according to the appearance and attitude scale (grade number), as shown in Supplementary Table S2. The omentum and bioreactor groups had significantly higher scores than the other groups in 1 week but rapidly decreased at ~15 days postoperatively (Fig. 3F, G). Consequently, all rats died within 15 days after the procedure due to a nutritional problem and airway obstruction. Although the animals could consume their liquid diet freely up to ~1 week, mechanical obstruction at their reconstructed esophagus developed as the regeneration process proceeded (hairball at the stenotic area or obstruction by the scaffold debris).

This phenomenon was inevitable because of the small diameter of the esophagus and lack of peristalsis after non-dynamic scaffold implantation. In all cases, we found that hairballs caused complete obstruction of the reconstructed proximal esophagus. We could not maintain the weight over 300 g with gastrostomy feeding after complete obstruction of the reconstructed esophagus. We speculate that the airway obstruction caused by the saliva and ingested materials, which could not be swallowed, caused systematic severe complications with continuous weight loss. However, hMSC inoculation and several technical enhancements confirmed

that esophageal reconstruction could be possible in the circumferential esophageal defects model.

Blood parameters

The values obtained for blood parameters, including BUN, WBC, Hgb, and Alb at 7 and 14 days after the surgery, are shown in Figure 4. BUN is associated with dehydration of the animal body.[16] The control group showed severe dehydration that, in turn, may decrease their resistance to bacteria. This group also had a significantly higher WBC value than the other experimental group. We can infer this was because of an inflammatory response in the transplanted regions. Particularly, the flap group showed a slight increase in the WBC value at 14 days. Hgb is another key parameter that is related to anemia.[17] Anemia can also be caused by not supplying the correct nutrients. The omentum and bioreactor groups showed significantly higher Hgb levels than the MSC and control groups. However, the Hgb value of all the groups decreased to a certain level over time. Additionally, a low Alb level is caused by stress or nutritional deficiency. A significantly higher level of Alb was detected in the three experimental groups (MSC, omentum, and bioreactor groups) up to 7 days, whereas the levels in all the experimental groups returned to a low level at 14 days.

Reepithelialization and cell tracking in implanted sites

An autopsy was immediately conducted to confirm the cause of death, and the cervical esophagus was harvested via total laryngopharyngoesophagectomy. The harvested tissue included a whole length of the cervical esophageal tissues. Most of the scaffold-transplanted rats without a thyroid gland flap died within 5–8 days due to leakage on the anastomosis site. Loose integration between the distal end of the scaffold and host tissue was confirmed by the H&E staining of the control group (Fig. 5, black arrows). After thyroid gland flap surgery, anastomosis fistulas were not observed. However, scaffold fragments were frequently observed in most of the anastomosis sites (Fig. 5, red arrows). This result indicates that the structure of the scaffold eventually collapsed during the wound healing process. Nevertheless, the omentum and bioreactor groups could confirm the connectivity of the esophageal lumen. Most experimental rats without anastomosis leak survived to 15 days. Although the animals of the omentum and bioreactor groups developed neoesophageal obstruction by hairball, there was no gross evidence of perforation, fistula, seroma accumulation, abscess formation, or surrounding soft tissue necrosis in all the experimental rats.

Immunofluorescence staining for Keratin-13 was carried out to identify reepithelialization in the reconstructed esophageal layer (Fig. 6A). Although no regenerated mucosal layer was observed around the implants of the control group, more than 80% of the mucosal regeneration was observed in the omentum and bioreactor groups (Fig. 6B). It was clear that omentum culture and bioreactor system had a critical effect in promoting mucosal regeneration. We next examined whether hMSCs survived *in vivo* via human nuclei immunostaining (Fig. 6C). The hMSCs strongly expressed red fluorescence around the 3D printed PCL strand (marked by a white star), suggesting that the transplanted cells remained stable at the transplantation site.

Expression of elastin fiber and collagen at implanted sites

Elastin and collagen fiber deposition was observed in all parts of the artificial esophagus (Fig. 7). Collagen deposition was weakly stained around the implanted site in the control group, whereas all the groups covered with the thyroid gland flap tightly increased collagen deposition surrounding grafts (Fig. 7A). In addition, the elastin fiber with distinct morphology was exhibited in all the MSC-seeding groups (Fig. 7B). Particularly, the histological morphology of elastin

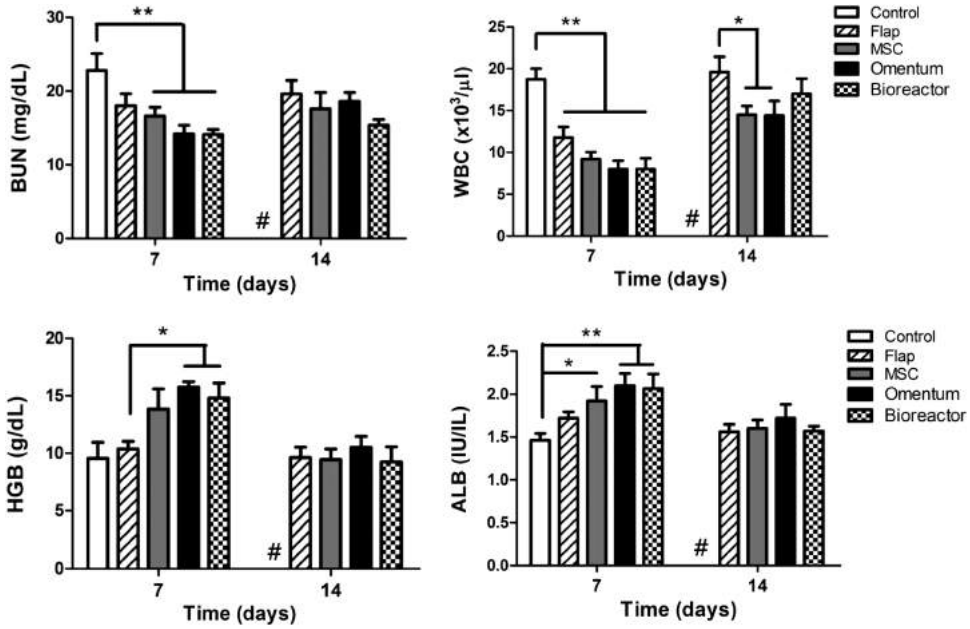

FIG. 4. Postoperative blood parameters. The values obtained from the blood parameters in the omentum and bioreactor groups did not show any significant evidence of dehydration or malnutrition until the first week after the surgery. However, all the parameters deteriorated to similar levels with the other experimental groups after second weeks. $^{*}p < 0.05$ or $^{**}p < 0.01$. The control group did not survive for more than 7 days (#).

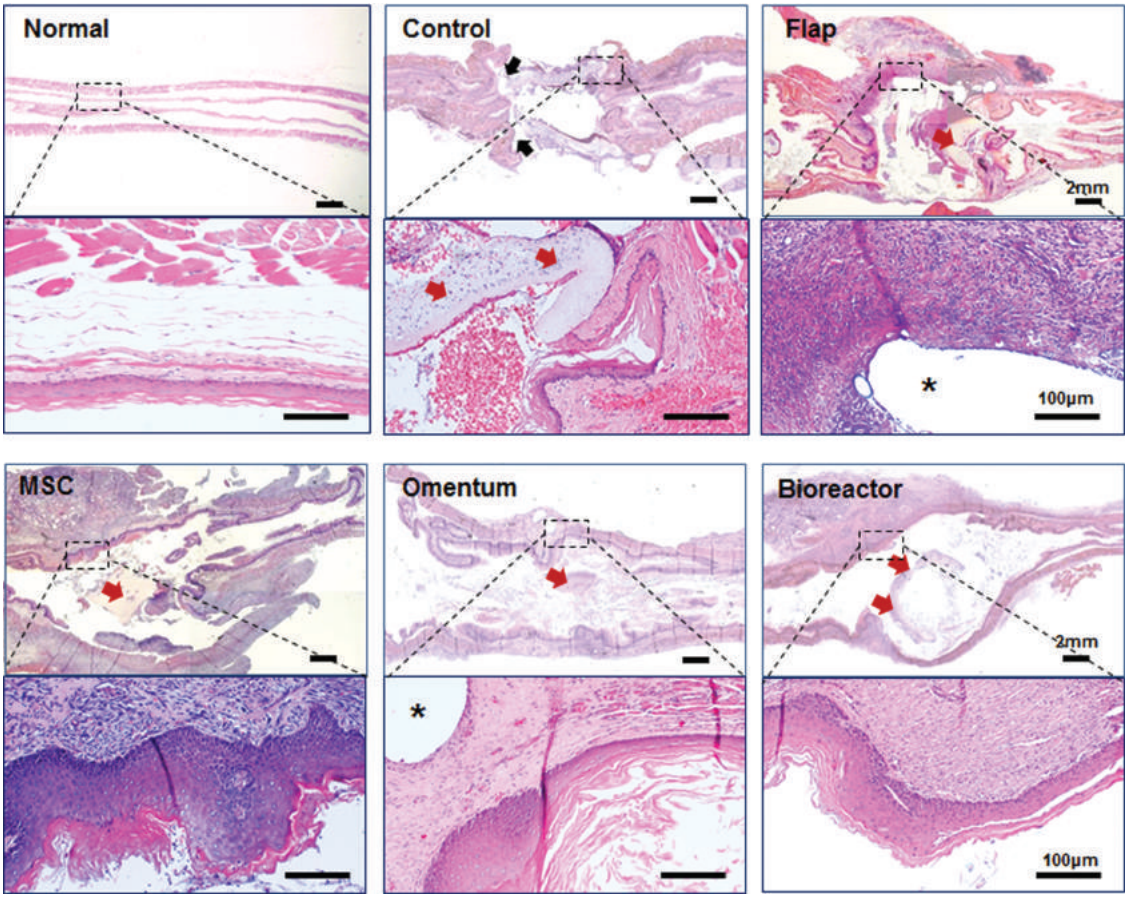

FIG. 5. Whole histology of the reconstructed esophagus 2 weeks after orthotopic scaffold implantation. The control group showed no signs of tissue regeneration around the graft, and leakage was clearly observed at the distal portion (*black arrows*). Particularly, the omentum and bioreactor groups showed complete healing of the circumferential defects. Broken scaffold debris was intermittently observed inside the esophagus (*red arrows*). (*, PCL strand). Color images are available online.

fiber in the omentum and bioreactor groups was also similar to that of the normal group. The presence of abundant elastin and collagen fibers could contribute toward better mechanical properties.

Regeneration of esophageal muscle

Desmin immunostaining was conducted to estimate whether the hMSC-seeded tubular scaffold including the surgical techniques can induce esophageal muscle regeneration around the implanted site. From the result, it was observed that the flap and MSC groups intermittently showed a strong green color (arrows) around the implanted sites, indicating muscle regeneration (Fig. 8A). Particularly, muscle regeneration was significantly increased in the omentum and bioreactor groups compared with the other two experimental groups (Fig. 8B). By contrast, the control group showed no signs of regenerated esophageal muscle.

Neovascularization and inflammatory responses in the implanted sites

Von Willebrand factor, a blood vessel-specific marker, immunostaining was performed to identify the formation of new blood vessels at the transplanted sites of each group. A representative immunohistochemical image with blood vessels shown in brown is shown in Figure 9A. Neovascularization was rarely observed in the graft site of the control group. However, the omentum and bioreactor groups led to a significantly higher number of blood vessels than those of the MSC group (Fig. 9B).

Immunohistochemical analysis for F4/80 reflected macrophage infiltration at the transplanted site (Fig. 9C). The macrophage activation (DAB-positive stains; arrows) associated with inflammation was higher in the naked scaffold group and was significantly reduced in the hMSC-treated group at 2 weeks (Fig. 9D). These results suggest that immunomodulation could be developed in the hMSC-treated group.

Discussion

Current treatments of esophageal diseases, such as congenital anomalies and esophageal cancer, require the removal of a significant portion of the disease area, but the esophagus is a specialized organ with peristalsis that cannot regenerate. Unfortunately, conventional standard esophageal reconstruction with the stomach, jejunum, or colon is associated with a wide range of complications and

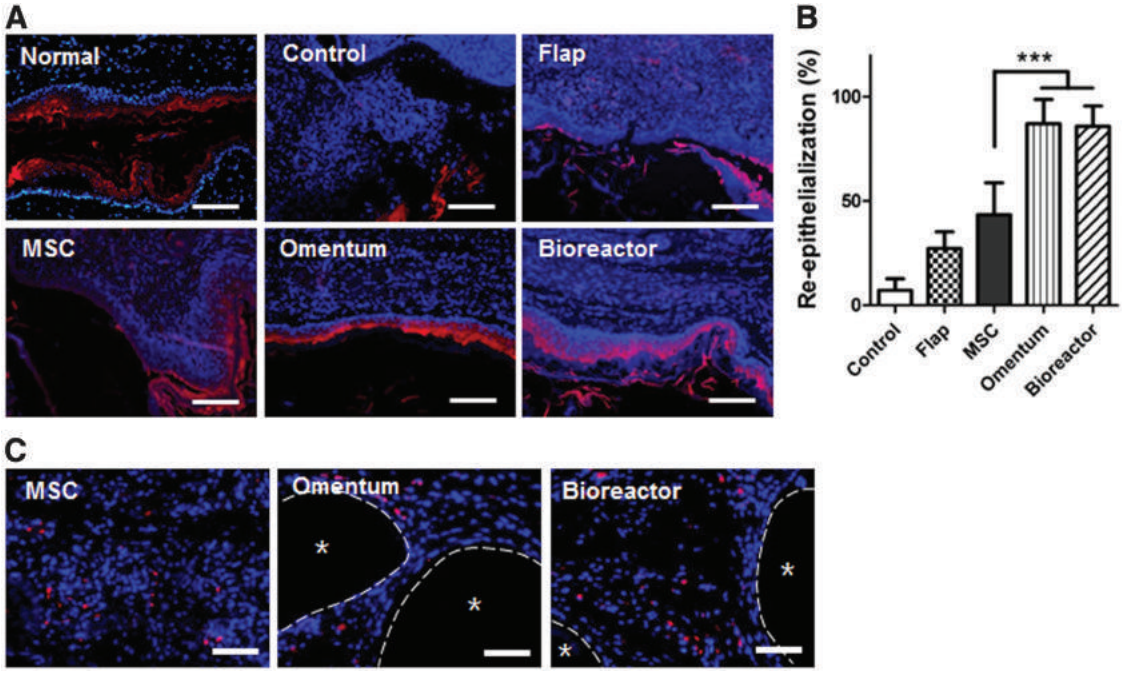

FIG. 6. Reepithelialization of the reconstructed esophagus 2 weeks after orthotopic scaffold implantation. **(A)** Keratin-13 immunostaining exhibited regenerative esophageal epithelium at 2 weeks after implantation. The omentum and bioreactor groups showed continuous and strong signals for Keratin-13 in the regenerative mucosal layer. Each image indicated the *dotted square* in Figure 5A. **(B)** Quantitative analysis of the reepithelialization 2 weeks after the surgery (***$p < 0.001$). The omentum and bioreactor groups showed significantly greater reepithelialization than the MSC groups. **(C)** Immunohistochemistry using anti-human nuclei antibodies for cell tracking. Human nuclei-positive cells were revealed around the implanted scaffold (*, PCL strand) in all hMSC-seeded groups. Color images are available online.

morbidity.[18,19] Various substitutes have been utilized for esophageal tissue engineering. Certainly, acellular allografts/xenografts/decellularized esophageal grafts, which have native structures and components, have shown the best regeneration results.[4,20,21] However, these substitutes are inherently exposed to disease transmission and immunogenicity problems. Additionally, commercialization is difficult, and mechanical properties are generally weak. Furthermore, nonabsorbed scaffolds, such as silicone, have been used for esophageal regeneration; however, these substitutes require a postoperation for removal and are associated with various postsurgery complications.[22] Therefore, nondegradable constructs with biomimetic structures and mechanical properties are other alternatives. Esophageal tissue engineering with natural or synthetic biomaterials that are designed for each patient can be a more feasible alternative therapy than conventional treatments.[23,24]

However, conventional animal research on the artificial esophagus is challenging due to several critical factors. The ideal esophageal substitute should also be biocompatible, and the scaffold should support the adhesion, infiltration, and proliferation of each epithelial cell, fibroblast, and smooth muscle cell and not cause infection and inflammation. Mechanical characteristics of the esophagus are essential because the esophagus is collapsed at the time of respiration and open during the swallowing process with constant exposure to maximal stretching with a recoil phenomenon. Hence, the implanted scaffold must have characteristics similar to the native organ. The viscoelasticity of the implanted esophagus should be adequate for repetitive ramp-relaxation of the peristaltic movement through the esophagus. The burst and dilation strength of the scaffold should match the native esophagus because it should neither shrink nor leak.[7,8] Scaffolds that are too weak may rupture or leak and cause severe conditions, such as mediastinitis, in the recipient. By contrast, a scaffold that is too stiff could bulge into the esophageal lumen and prevent food passage.

Electrospinning has been introduced as a suitable method to fabricate scaffolds that mimic the native extracellular matrix (ECM) in the human body. However, any scaffolds manufactured from electrospun nanofibers have limitations in artificial esophagus applications due to their poor mechanical properties.[8,25] To solve this problem, we propose a hybrid technology involving sequential outer filaments to improve mechanical properties using the 3D printing technique to produce a hybrid tubular scaffold. Combining electrospinning and the 3D printing technique could improve the ability to engineer multifunctional composite tubular organ scaffolds. This hybrid tubular scaffold allows excellent mechanical properties compared with pristine electrospun grafts (Fig. 2C).[26] When we compared the compliance of our artificial scaffold and native tissue, we observed a significantly smaller compliance of the scaffold. This might be caused by a lack of cell and ECM components and might be improved by cell seeding and culture. According to a previous study, the mechanical property of scaffold could be improved after implantation.[24] Regrettably, the samples prepared for implantation were too short in length for compliance testing in present study. However,

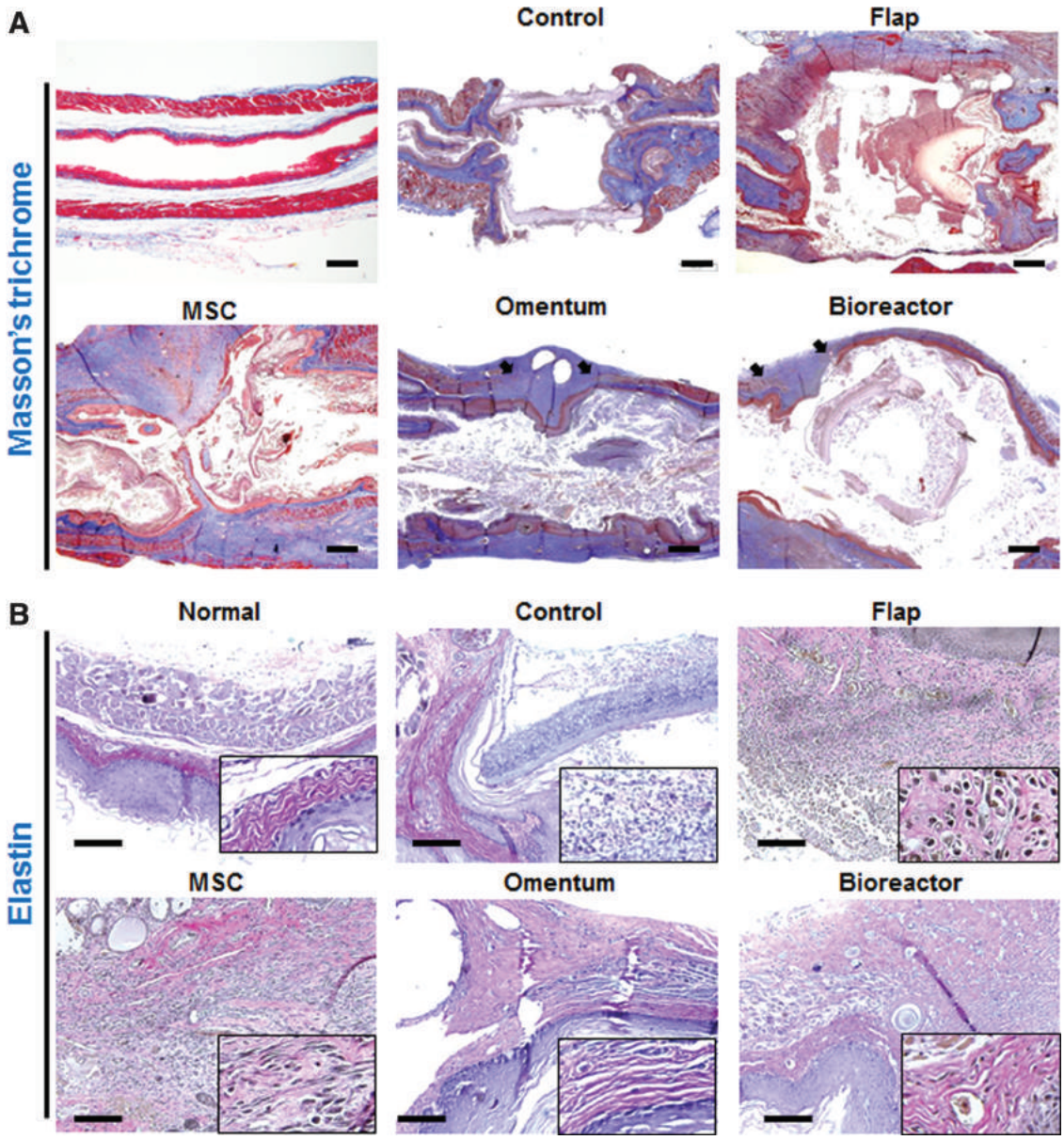

FIG. 7. Production of collagen and elastin fiber at the implanted sites. **(A)** Masson's trichrome staining shows the tendency of collagen deposition around the implanted sites for each group. **(B)** The regeneration of elastin fiber, indicating the mechanical elasticity of esophageal tissue, was confirmed by elastin immunostaining. In the omentum and bioreactor groups, elastin fibers with morphology similar to normal were abundantly observed. Color images are available online.

we conducted a related *in vitro* experiment, which showed the compliance of scaffold increased after cell seeding and approximately increased by 27% and 49% in steady culture and pulsatile bioreactor groups, respectively (Supplementary Fig. S2). Therefore, based on those results, we assumed that the compliance of the substitute after implantation might be similar to that of the native tissue due to the regeneration of epithelial and muscular components. The 3D printed strand in the outer layer had a width of 780 μm, which was considerably wider inside space. It focuses on the physical role of support for esophageal peristalsis rather than the role of induction of surrounding tissue. In fact, scaffolds have extremely high modulus of elasticity and maximum stresses compared with their esophagus (Fig. 2C). Unfortunately, it is not easy to mimic the soft elasticity of real muscle tissue as a synthetic polymer. To mimic the peristaltic motion of the esophageal muscle tissue, a suitable combination with natural polymers (e.g., collagen, gelatin, alginate, and hyaluronic acid) could be another option. The inner layer of nanofibers prevents infiltration of various bacteria and provides moderately tough properties. In addition, nanosized fibers provide a topographical cue that mimics ECM and have a beneficial effect on initial mucosal formation and proliferation of inoculated cells.

Circumferential reconstruction of the esophagus by a completely acellular matrix, which is used alone without cell seeding, invariably leads to the absence of tissue remodeling and stricture formation.[8] Early formation of the

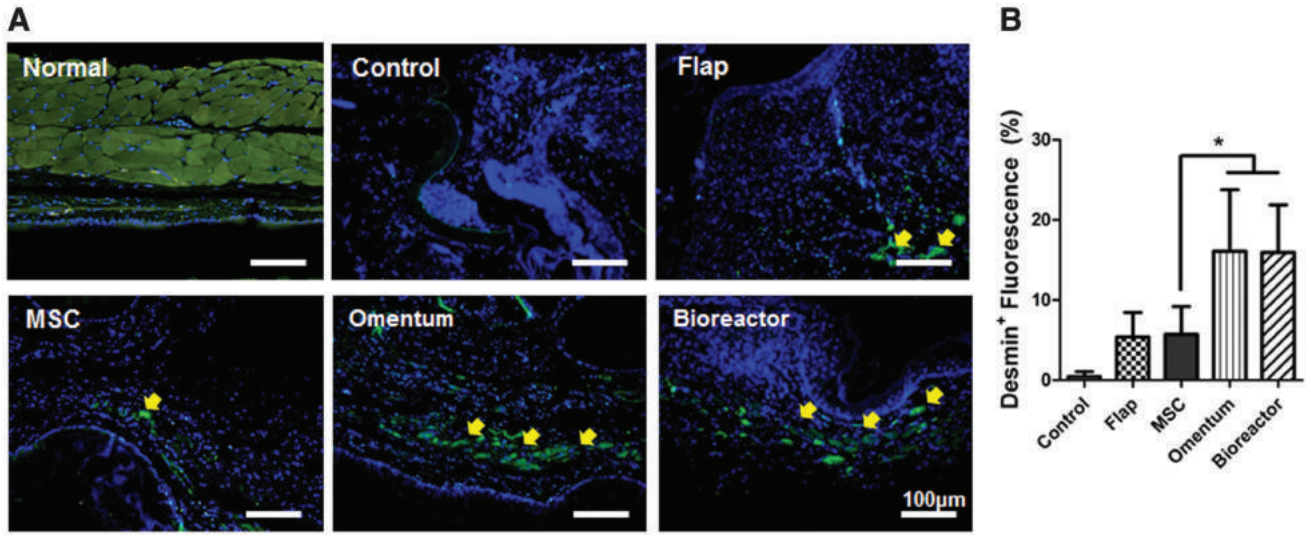

FIG. 8. Regeneration of esophageal muscle at implanted sites. **(A)** Representative images of desmin immunostaining in the reconstructed esophagus after the surgery. Desmin-positive signals exhibited newly regenerated muscle adjacent to the implanted sites (*yellow arrows*). **(B)** Quantitative analysis of the desmin-positive area. $*p < 0.05$. Color images are available online.

mucosal layer before stenosis can be a critical strategy for esophageal reconstruction.[27] Cell grafts at the inner wall of the tubular scaffold might be a key factor in initial mucosal formation. We used human adipose-derived MSCs to promote early mucosal formation. Many studies have previously reported on the efficacy of MSCs for mucosal regeneration.[8,28,29] Additionally, clinical interest in MSCs has been increasing because MSCs have immune privileges and, more importantly, immunoregulatory ability.[30–32] Although the mechanisms underlying the immunosuppressive effect of MSCs have not been clearly defined, they have been previously used in various animal models.[33–35] Based on these technical theories, we applied human-derived MSCs to esophageal regeneration studies. We previously confirmed that hMSC-seeded tubular scaffolds exhibited greater cell adhesion and epithelial differentiation efficiency than naked tubular scaffolds in bioreactor culture.[15] Dynamic culture before implantation has significant advantages for cell adhesion and early epithelial differentiation. Extension of the *in vitro* culture time or further application of circumferential mechanical forces by the bioreactor might help the regeneration of the esophageal muscular layer, enhance peristaltic function, and solve the obstruction problem afterward. We demonstrated the effect of 3D tubular scaffolds and dynamic culture conditions on esophageal reconstruction. Histological evaluations also showed excellent reepithelialization of the circumferential defect site in the bioreactor group (Fig. 6A). However, there are several critical variables in addition to cell seeding that could be implicated in the ultimate integrity of the esophageal scaffold, including scaffold selection, peri/postoperative nutrition technique, scaffold anastomosis technique, and adequate blood supply to the implanted scaffold.

Anastomosis site leakage and necrosis of the implanted substitutes inevitably cause serious complications because of the neck and mediastinal space contamination.[36] Many vital organs are located in these spaces, and infection or necrosis of these vital structures constitutes a significant cause of mortality. Therefore, it is imperative to prevent food or saliva accumulation in the reconstructed surgical wound, and a nasogastric tube should be inserted for bypass feeding in the first or second postoperative week. To date, there are no established bypass feeding methods (such as nasogastric tube or gastrostomy) to supply nutrients in adult rats because researchers could not maintain the feeding tube in the adult rat stomach for a long time due to the rats being extremely active and uncontrollable. In this study, we applied our new gastrostomy technique for optimal peri/postoperative nutrition (Fig. 3A).

The anastomosis technique using a small diameter of the rat esophagus is not well established. The conventional suture technique using the naked eyes cannot achieve a watertight suture for the rat model. We applied the microvascular anastomosis technique to esophageal scaffold implantation to improve surgical completeness. Angiogenesis is a fundamental process for wound healing, functional recovery, and new organ development. Moreover, it prevents graft failure of the transplanted artificial scaffold. However, once the artificial scaffold is transplanted *in vivo*, it should be alive in the initial stage through the diffusion of various nutrients and oxygen. Therefore, a reliable vascular vehicle for the delivery of nutrients, growth factors, and oxygen is required during this initial stage.[9] The thyroid gland is a vascular tissue located near the esophagus.[37] The introduction of vascularized tissue from surrounding tissue decreases the risk of major wound complications after laryngopharyngoesophageal surgery in humans. This has been shown to prevent or reduce the risk of fistula and leakage from the anastomosis site. The use of the vascularized thyroid gland flap is one of the reconstructive methods after laryngectomy, and we used the thyroid gland flap after circumferential esophagectomy because of its easy accessibility in a rat model.[38] This is the first study to assess the rat model for circumferential esophageal defect reconstruction using a hybrid scaffold, gastrostomy, a microscopic anastomosis technique, and a thyroid gland flap in a

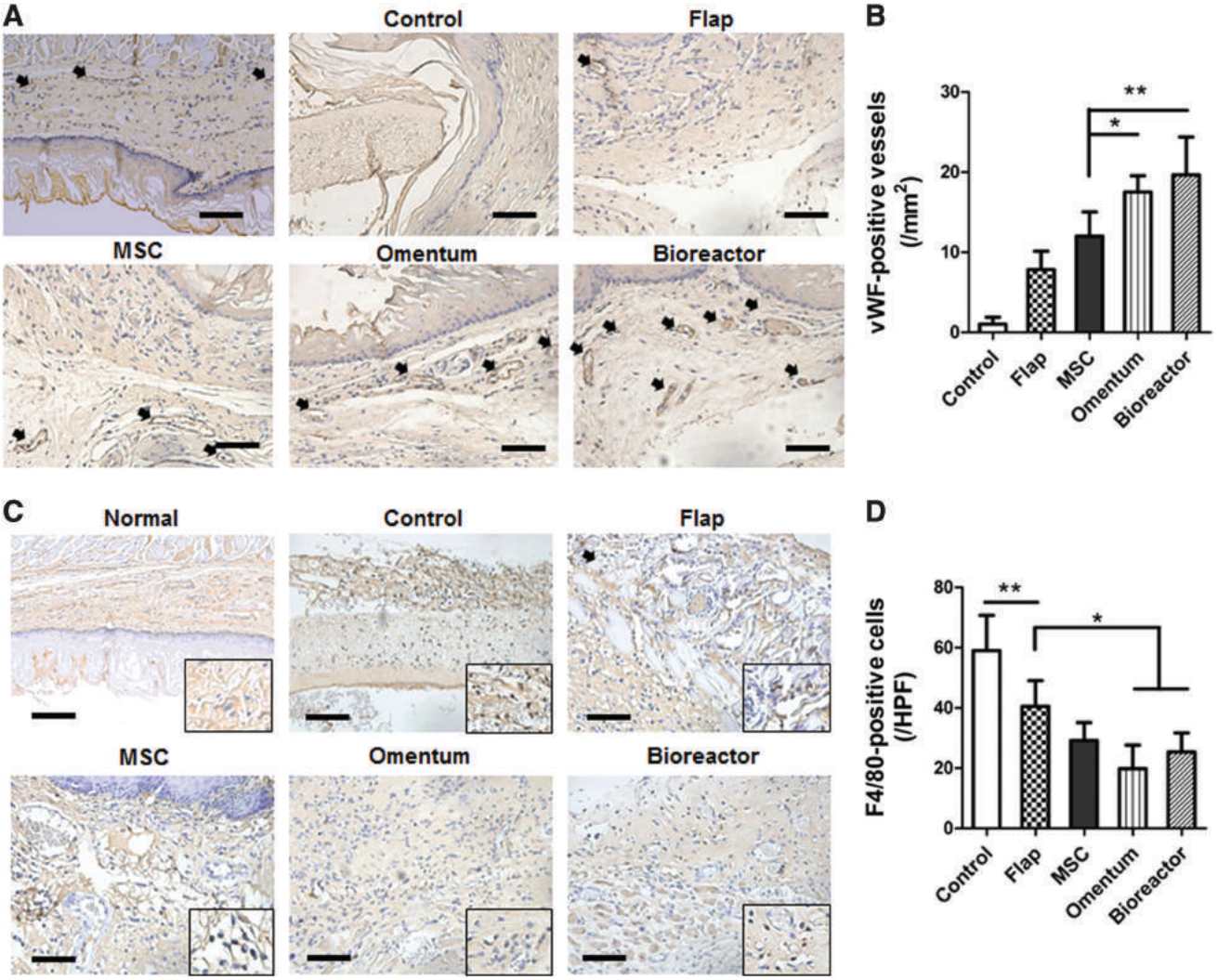

FIG. 9. Immunohistochemical staining of blood vessels and macrophages at 2 weeks after implantation. **(A)** Representative image showing the regenerated blood vessel by vWF expression. The *arrows* represent vWF-positive vessels. **(B)** Statistical analysis of the number of vWF-positive blood vessels per square millimeter. **(C)** Representative image showing the infiltration of macrophages by F4/80 expression. The *arrows* represent F4/80-positive vessels. **(D)** Statistical analysis of the number of F4/80-positive macrophages per high-power field. Particularly, macrophage expression in the omentum and bioreactor groups were significantly decreased compared with that in the flap group. $*p < 0.05$ or $**p < 0.01$. vWF, von Willebrand factor. Color images are available online.

bioreactor cultivation environment. However, a small animal model for circumferential esophageal defects is technically challenging in many aspects. Meanwhile, large animal models (i.e., dogs) undergoing circumferential esophageal defect reconstruction are technically easier. The size of their esophagus is bigger, which allows easier surgical implantation and continuous food passage, even without local peristalsis. Moreover, large animals can be fed only by intravenous hyperalimentation for 2 to 4 weeks after implanting the prosthesis.[39,40] In previous studies, we focused on improving esophageal tissue organization through omentum-cultured tubular scaffolds.[10] In fact, the omentum-cultured system is an important clinical technique for early vascular supply for tissue regeneration of naked scaffolds.[9,41–43] It was also technically expected to minimize the collapse of the scaffold. However, the use of the omentum-cultured technique in clinical practice is associated with complications due to additional surgery. In the present study, although the circumferential esophageal defects were completely healed by the second week in this group, all the experimental rats died before the 15th postoperative day. The deaths occurred due to malnutrition and leakage at the proximal site of anastomosis because of stenosis and graft obstruction by foreign material. Although all animals consumed their liquid diet freely for up to ~1 week, mechanical obstruction of the reconstructed esophagus developed as the regeneration process proceeded. This phenomenon is presumably due to the inability of peristalsis after insertion of nondynamic scaffold. In all cases, we observed that hairballs caused the complete obstruction of the reconstructed proximal esophagus. We speculate that airway obstruction caused by saliva and ingested materials that could not be swallowed caused serious systematic complications and continuous weight loss. We clearly understood the current problem. For

its clinical application, it is necessary to develop a scaffold of physical properties close to the native esophagus. In addition, an additional method of promoting tissue regeneration in harsh environments should be established.

Conclusion

In this article, we have described an innovative method for esophageal reconstruction in a rat model of a circumferential esophageal defect. Our findings showed that a bioreactor-cultured artificial esophagus can regenerate into esophageal mucosa and muscle similar to the omentum-cultured group. Future studies using large animal subjects are required to further understand the role of esophageal muscle and mucosal regeneration in circumferential esophageal reconstruction.

Acknowledgments

This research was supported by the Korea Health Technology R&D Project through the Korea Health Industry Development Institute (KHIDI), funded by the Ministry of Health & Welfare, Republic of Korea (grant number: HI16C0362).

Disclosure Statement

No competing financial interests exist.

Supplementary Material

Supplementary Data
Supplementary Figure S1
Supplementary Figure S2
Supplementary Table S1
Supplementary Table S2
Supplementary Video S1
Supplementary Movie S1

References

1. Irino, T., Tsekrekos, A., Coppola, A., *et al.* Long-term functional outcomes after replacement of the esophagus with gastric, colonic, or jejunal conduits: a systematic literature review. Dis Esophagus **30,** 1, 2017.
2. Flanagan, J.C., Batz, R., Saboo, S.S., *et al.* Esophagectomy and gastric pull-through procedures: surgical techniques, imaging features, and potential complications. Radiographics **36,** 107, 2016.
3. Catry, J., Luong-Nguyen, M., Arakelian, L., *et al.* Circumferential esophageal replacement by a tissue-engineered substitute using mesenchymal stem cells: an experimental study in mini pigs. Cell Transplant **26,** 1831, 2017.
4. Wang, F., Maeda, Y., Zachar, V., Ansari, T., and Emmersen, J. Regeneration of the oesophageal muscle layer from oesophagus acellular matrix scaffold using adipose-derived stem cells. Biochem Biophys Res Commun **503,** 271, 2018.
5. Chung, E.J., Ju, H.W., Park, H.J., and Park, C.H. Three-layered scaffolds for artificial esophagus using poly(E-caprolactone) nanofibers and silk fibroin: an experimental study in a rat model. J Biomed Mater Res A **103,** 2057, 2015.
6. Lopes, M.F., Cabrita, A., Ilharco, J., *et al.* Esophageal replacement in rat using porcine intestinal submucosa as a patch or a tube-shaped graft. Dis Esophagus **19,** 254, 2006.
7. Kuppan, P., Sethuraman, S., and Krishnan, U.M. Tissue engineering interventions for esophageal disorders—promises and challenges. Biotechnol Adv **30,** 1481, 2012.
8. Park, S.Y., Choi, J.W., Park, J.K., *et al.* Tissue-engineered artificial oesophagus patch using three-dimensionally printed polycaprolactone with mesenchymal stem cells: a preliminary report. Interact Cardiovasc Thorac Surg **22,** 712, 2016.
9. Suh, S., Kim, J., Shin, J., *et al.* Use of omentum as an in vivo cell culture system in tissue engineering. ASAIO J **50,** 464, 2004.
10. Chung, E.J., Ju, H.W., Yeon, Y.K., *et al.* Development of an omentum-cultured oesophageal scaffold reinforced by a 3D-printed ring: feasibility of an in vivo bioreactor. Artif Cells Nanomed Biotechnol **15,** 1, 2018.
11. Lee, S.J., Heo, D.N., Park, J.S., *et al.* Characterization and preparation of bio-tubular scaffolds for fabricating artificial vascular grafts by combining electrospinning and a 3D printing system. Phys Chem Chem Phys **17,** 2996, 2015.
12. Kim, D.H., Heo, S.J., Kang, Y.G., Shin, J.W., Park, S.H., and Shin, J.W. Shear stress and circumferential stretch by pulsatile flow direct vascular endothelial lineage commitment of mesenchymal stem cells in engineered blood vessels. J Mater Sci Mater Med **27,** 60, 2016.
13. Factor, P., Ridge, K., Alverdy, J., and Sznajder, J.I. Continuous enteral nutrition attenuates pulmonary edema in rats exposed to 100% oxygen. J Appl Physiol **89,** 1759, 1985.
14. Bekkevold, C.M., Robertson, K.L., Reinhard, M.K., Battles, A.H., and Rowland, N.E. Dehydration parameters and standards for laboratory mice. J Am Assoc Lab Anim Sci **52,** 233, 2013.
15. Wu, Y., Kang, Y.G., Cho, H., Kim, I.G., Chung, E.J., and Shin, J.W. Combinational effects of mechanical forces and substrate surface characteristics on esophageal epithelial differentiation. J Biomed Mater Res A **107,** 552, 2019.
16. Yoshihara, A., Hirotomi, T., Takano, N., Kondo, T., Hanada, N., and Miyazaki, H. Serum markers of chronic dehydration are associated with saliva spinability. J Oral Rehabil **34,** 733, 2007.
17. Sinha, N., Mishra, T.K., Singh, T., and Gupta, N. Effect of iron deficiency anemia on hemoglobin A1c levels. Ann Lab Med **32,** 17, 2012.
18. Wormuth, J.K., and Heitmiller, R.F. Esophageal conduit necrosis. Thorac Surg Clin **16,** 11, 2006.
19. Kim, S.H., Lee, K.S., Shim, Y.M., Kim, K., Yang, P.S., and Kim, T.S. Esophageal resection: indications, techniques, and radiologic assessment. Radiographics **21,** 1119, 2001.
20. Badylak, S.F., Vorp, D.A., Spievack, A.R., *et al.* Esophageal reconstruction with ECM and muscle tissue in a dog model. J Surg Res **128,** 87, 2005.
21. Luc, G., Charles, G., Gronnier, C., *et al.* Decellularized and matured esophageal scaffold for circumferential esophagus replacement: proof of concept in a pig model. Biomaterials **175,** 1, 2018.
22. Yamamoto, Y., Nakamura, T., Shimizu, Y., *et al.* Intrathoracic esophageal replacement with a collagen sponge—silicone double layer tube: evaluation of omental-pedicle wrapping and prolonged placement of an inner stent. ASAIO J **46,** 734, 2000.
23. La Francesca, S., Aho, J.M., Barron, M.R., *et al.* Long-term regeneration and remodeling of the pig esophagus after circumferential resection using a retrievable synthetic scaffold carrying autologous cells. Sci Rep **8,** 4123, 2018.

24. Urbani, L., Maghsoudlou, P., Milan, A., *et al.* Long-term cryopreservation of decellularised oesophagi for tissue engineering clinical application. PLoS One **12,** e0179341, 2017.
25. Ghasemi-Mobarakeh, L., Prabhakaran, M.P., Morshed, M., Nasr-Esfahani, M.H., and Ramakrishna, S. Electrospun poly(epsilon-caprolactone)/gelatin nanofibrous scaffolds for nerve tissue engineering. Biomaterials **29,** 4532, 2008.
26. Badylak, S., Meurling, S., Chen, M., Spievack, A., and Simmons-Byrd, A. Resorbable bioscaffold for esophageal repair in a dog model. J Pediatr Surg **35,** 1097, 2000.
27. Ohki, T., Yamato, M., Ota, M., *et al.* Prevention of esophageal stricture after endoscopic submucosal dissection using tissue-engineered cell sheets. Gastroenterology **143,** 582, 2012.
28. Lee, D.Y., Kim, H.B., Shim, I.K., Kanai, N., Okano, T., and Kwon, S.K. Treatment of chemically induced oral ulcer using adipose-derived mesenchymal stem cell sheet. J Oral Pathol Med **46,** 520, 2017.
29. Lee, D.Y., Lee, J.H., Ahn, H.J., *et al.* Synergistic effect of laminin and mesenchymal stem cells on tracheal mucosal regeneration. Biomaterials **44,** 134, 2015.
30. Marigo, I., and Dazzi, F. The immunomodulatory properties of mesenchymal stem cells. Semin Immunopathol **33,** 593, 2011.
31. Nauta, A.J., and Fibbe, W.E. Immunomodulatory properties of mesenchymal stromal cells. Blood **15,** 3499, 2007.
32. Li, C.L., Leng, Y., Zhao, B., *et al.* Human iPSC-MSC-derived xenografts modulate immune responses by inhibiting the cleavage of caspases. Stem Cells **35,** 1719, 2017.
33. Lee, S.Y., Kwon, B., Lee, K., Son, Y.H., and Chung, S.G. Therapeutic mechanisms of human adipose-derived mesenchymal stem cells in a rat tendon injury model. Am J Sports Med **45,** 1429, 2017.
34. Suenaga, H., Furukawa, K.S., Suzuki, Y., Takato, T., and Ushida, T. Bone regeneration in calvarial defects in a rat model by implantation of human bone marrow-derived mesenchymal stromal cell spheroids. J Mater Sci Mater Med **26,** 254, 2015.
35. Liu, X., Chen, W., Zhang, C., *et al.* Co-seeding human endothelial cells with human-induced pluripotent stem cell-derived mesenchymal stem cells on calcium phosphate scaffold enhances osteogenesis and vascularization in rats. Tissue Eng Part A **23,** 546, 2017.
36. Huang, K., Wu, B., Ding, X., Xu, Z., and Tang, H. Post-esophagectomy tube feeding: a retrospective comparison of jejunostomy and a novel gastrostomy feeding approach. PLoS One **9,** e89190, 2014.
37. Ikeda, A., Okamoto, H., Tsuchiya, Y., Nishimura, K., Ueda, H., and Ogawa, T. Case of partial vertical laryngectomy with vocal cord reconstruction using a thyroid gland flap. Head Neck **36,** 73, 2014.
38. Yeh, D.H., Sahovaler, A., and Fung, K. Reconstruction after salvage laryngectomy. Oral Oncol **75,** 22, 2017.
39. Chung, E.J. Bioartificial esophagus: where are we now?. Adv Exp Med Biol **1064,** 313, 2018.
40. Londono, R., and Badylak, S.F. Regenerative medicine strategies for esophageal repair. Tissue Eng Part B Rev **21,** 393, 2015.
41. Messineo, A., Filler, R.M., Bahoric, B., Smith, C., and Bahoric, A. Successful tracheal autotransplantation with a vascularized omental flap. J Pediatr Surg **26,** 1296, 1991.
42. Soffer-Tsur, N., Shevach, M., Shapira, A., Peer, D., and Dvir, T. Optimizing the biofabrication process of omentum-based scaffolds for engineering autologous tissues. Biofabrication **6,** 035023, 2014.
43. Li, J., Xu, P., Chen, H., Yang, Z., and Zhang, Q. Improvement of tracheal autograft polyamide-6. Improvement of tracheal autograft survival with transplantation into the greater omentum. Ann Thorac Surg **60,** 1592, 1995.

Address correspondence to:
Jung-Woog Shin, PhD
Department of Biomedical Engineering
Inje University
Gimhae 621–749
Republic of Korea

E-mail: biomechshin@gmail.com

Eun-Jae Chung, MD, PhD
Department of Otorhinolaryngology-Head and Neck Surgery
Seoul National University College of Medicine
Seoul 03080
Republic of Korea

E-mail: voicechung@snu.ac.kr

Received: September 22, 2018
Accepted: February 19, 2019
Online Publication Date: May 10, 2019